Letters in Applied NanoBioScience
Platinum Open Access Journal (ISSN: 2284-6808)

Article
Volume 11, Issue 4, 2022, 3989 - 4006
https://doi.org/10.33263/LIANBS114.39894006

Design and Development of Complexation of Ce^{+3} Metal Ions with Synthesized INZ Incorporated Bio-active Schiff Bases

Zamzam Taher Omer (Al-Ahdal) [1], Megha Rai [1,*], Pravin Chavan [2,*], Rashmi Pathrikar [3], Shivaji Jadhav [4,*]

[1] Department of Chemistry, Dr. Rafiq Zakaria College for Woman, Aurangabad, 431001, (MS), India
[2] Department of Chemistry, Doshi Vakil College, Goregaon-Raigad, 402103, (MS), India
[3] Department of Chemistry, Rajashri Shahu College, Pathri-Aurangabad, 431111, (MS), India
[4] Department of Chemistry, Tarai College of Arts and Science, Paithan-Aurangabad, 431107, (MS), India
* Correspondence: dr.shivaji1985@gmail.com (S.J.), chemistryp141286@gmail.com (P.C.), drmegha08@gmail.com (M.R.);

Scopus Author ID 20433406800
Received: 24.08.2021; Revised: 20.10.2021; Accepted: 24.10.2021; Published: 30.10.2021

Abstract: In the present research, a series of Ce^{+3} metal ions complexation with INZ incorporating Schiff bases have been reported. INZ incorporated Schiff Bases (3a-e) were developed by condensing INZ with substituted aromatic aldehyde and confirmed with various spectral Techniques such as Elemental analysis, UV, IR, ^{1}H-NMR, ^{13}H NMR. All the synthesized organic ligands were evaluated against antibacterial and antifungal stains and found moderate to significant results. The Ce^{+3} metal ion solution mixed with newly prepared bio-active INZ Schiff bases (3a-e) to afford the [Ce-INZ Schiff Base] complexes (4a-e). The stability constants of prepared complexes were evaluated and found in order as a (3e) > (3d) > (3a) > (3b) > (3c).

Keywords: Ce^{+3} metal Complexes; INZ Schiff Base; stability constant; INZ; biological evaluation.

1. Introduction

Nowadays, the complexation of pharmacologically active Schiff bases plays a vital role in various areas of the medicinal field [1-14]. Schiff bases showed various applications, such as maintaining the carbonyl group oxidation state, which they used as heterocyclic organic components, stimulating several enzymes, easily manufacturing, and Cheapest. Complexes of transition metal ion with Heteroatom containing Schiff bases show several pharmaceuticals applications like antibacterial, antifungal, antituberculosis, ant-inflammatory, anticancer, antimalarial antiviral, and antioxidant activities [15-17]. Also, it's applicable in the field of agriculture, biochemistry, oxygenation, electron reduction, and catalytic synthesis [18, 19]. Inner transition metal/lanthanide ions also have a great capacity to perform coordination with heterocyclic compounds due to their vacant *f*-orbital. Lanthanides such as Sm (III) significantly form complexes with piperidin-4-ones [20]. Several biological applications (to stimulate metabolism in a living organism) of Silvery-white Sm metal ve attracted most researchers for its complexation study with heterocycles. Lanthanide complexation of coumarin-3-carboxylic acid (HCCA) shows significant antiproliferative activity [21]; it also has the appreciable capability to form stable complexes with Schiff bases which have various applications in

healthcare, clinical, and analytical fields [22, 23]. Due to its importance in healthcare fields, most researchers have been attracted to perform complexation of Schiff bases [24]. Isoniazid is one of the famous anti-tubercular agents [25, 26], stability and pharmacological application of INZ are enhanced by complexation. Drug complexes are more potent than parent drugs [27].

Due to these valuable findings of INZ and metal complexation Schiff bases in several fields, the author studied the preparation of inner transition Ce^{+3} ion complexes with INZ incorporated Schiff bases (3a-e).

2. Materials and Methods

2.1. Synthesis and characterizations.

2.1.1. Synthesis.

Schiff bases as ligand were successfully prepared via condensation of isoniazid (INZ) with substituted aromatic aldehydes in the presence of glacial acetic acid (GGA) as a catalyst in ethanol. All chemicals were commercially purchased from Sigma Aldrich Chemical Laboratory.

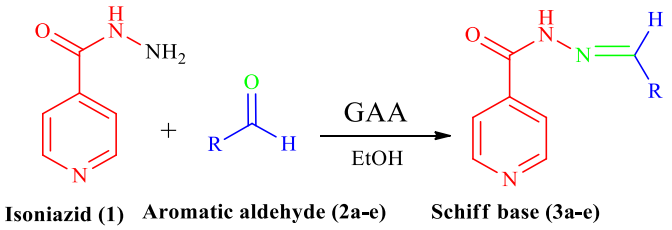

Scheme 1. Conjugated Schiff bases synthesized via condensation of INZ with Substituted Aromatic aldehyde.

Prepared organic ligands (3a-e) were confirmed by various spectroscopic techniques such as ^{13}C NMR, ^{1}H NMR, UV-Visible spectrophotometer, and IR. We observed single color spots of prepared Schiff bases on Thin Layer Chromatography plate using DMSO: EA (5:5).

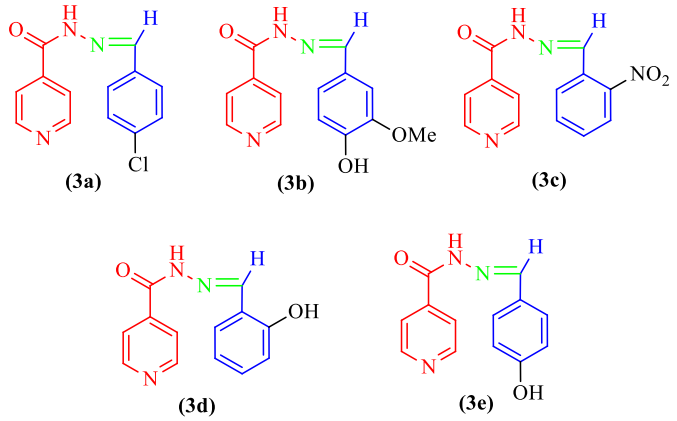

Scheme 2. Synthesized Schiff Bases (3a-e).

IR spectra were recorded on Brucker FT-IR device using KBr pellet. LECO CHNS - 932 micro analyzer instruments were used for elemental analysis. UV-Visible (SL 210 multipurpose in the range of 190-110 nm) instrument was used for prepared Schiff bases analysis. ^{1}H NMR spectra were recorded on the Bruker DRX-300 instrument, and ^{13}C NMR spectra were recorded on Bruker DRX-75, 100 MHz NMR instrument in DMSO/$CDCl_3$-*d6*.

2.1.2. Spectral analysis.

N-[(E)-(4-chlorophenyl) methylene]isonicotinohydrazide (3a)- Yield: 97 %, MP: 212-214^{o}C, Elemental analysis: molecular formula : $C_{13}H_{10}ClN_3O$, Mol. Wt. 259.69, Calculated C:60.23, H:3.86, N:16.21 Found C:60.19, H:3.83, N:16.17; The FTIR in (KBr cm^{-1}) : 3646-3444 (N-H stretching), 1664 (C=O), 1608 (C=N), 1486 (Ar, C=N), 1551 (Ar, C=C) (Figure S1). ^{1}H NMR (400 MHz, DMSO *d*$_6$) δ 11.97 (s, 1H, D_2O exchangeable NH), 8.40 (s, 1H, aliphatic), 8.70-8.69 (d, 2H, J=5.6 Hz, Pry-H), 7.77-7.76 (d, 2H, J=5.6 Hz, Ar-H), 7.70-7.68 (d, 2H, J=8.4 Hz, Pry-H), (7.36-7.34 (d, 2H, J=8.4 Hz, Ar-H) (Figure S2). ^{13}C NMR (100 MHz, DMSO *d*$_6$) 121.84, 129.07, 129.10, 133.09, 135.64, 140.70, 148.25, 150.43, 162.24 ppm(Figure S3). The UV–Visible absorbance peaks was shifted to a longer wavelength (lower frequency) observed at 306 nm(Figure S4).

N-[(E)-(4-Hydroxy-3-methoxyphenyl)isonicotinohydrazide (3b)- Yield: 98 %, MP: 230-232^{o}C; elemental analysis: molecular formula : $C_{14}H_{13}N_3O_3$, Mol. Wt. 271.27,Calculated C:60.23, H:3.86, N:16.21 Found C:60.19, H:3.83, N:16.17; The FTIR in (KBr cm^{-1}) : 3648-3445 (N-H stretching), 1698 (C=O), 1683 (C=N), 1550 (Ar, C=C), 1374 (Ar, C=N), 1224 (Ar, C-OH), 1128 (Ar, O-CH_3) (Figure S5). ^{1}H NMR (400 MHz, DMSO *d*$_6$) δ 11.78 (s, 1H, D_2O exchangeable NH), 9.30 (s, 1H, OH), 8.30 (s, 1H, aliphatic), 8.67-8.65 (d, 2H, J=6.4 Hz, Pry-H), 7.77-7.76 (d, 2H, J=3.2 Hz, Ar-H), 7.90 (d, 2H, J=2.4 Hz, Pry-H), 7.33 (s,1H, Ar-H), 3.82 (s,3H, OCH_3) (Figure S6). ^{13} C NMR (100 MHz, DMSO *d*$_6$): 109.20, 115.53, 121.82, 123.15, 125.70, 140.97, 149.68, 150.34, 162.01 ppm(Figure S7). The UV–Vis absorbance peaks was shifted to a longer wavelength (lower frequency) observed at 327 nm(Figure S8).

N-[(E)-(2-Nitrophenyl)methylene]isonicotinohydrazide (3c)- Yield: 99 %, MP: 235-237^{o}C; elemental analysis: molecular formula : $C_{13}H_{10}N_4O_3$, Mol. Wt. 270.24, Calculated C:57.75, H:3.70, N:20.73 Found: C:57.71, H:3.67, N:20.69; The FTIR in (KBr cm^{-1}) : 3646-3444 (N-H stretching), 1664 (C=O), 1608 (aliphatic C=N), 1486 (aromatic C=N), 1551 (Ar, C=C) (Figure S9). ^{1}H NMR (400 MHz, DMSO *d*$_6$) δ 12.32 (s, 1H, D_2O exchangeable NH), 8.72 (s, 1H, aliphatic), 8.94-8.93 (d, 2H, J=4.4 Hz, Pry-H), 8.72-8.71 (d, 2H, J=4 Hz, Ar-H), 8.18-8.17, (d, 2H, J=4.4 Hz, Pry-H), 8.16-8.15 (t, 2H, J =4 Hz, Ar-H) (Figure S10). ^{13} C NMR (100 MHz, DMSO *d*$_6$): 121.88, 124.87, 128.63, 129, 131.04, 133.87, 140.34, 144.73, 148.56, 150.50, 162.35 ppm(Figure S11). The UV–Visible absorbance peaks was shifted to a longer wavelength (lower frequency) observed at 275 nm(Figure S12).

N-[(E)-(2-Hydroxyphenyl)methylene]isonicotinohydrazide (3d)- Yield: 98 %, MP: 243-245^{o}C; elemental analysis: molecular formula: $C_{13}H_{11}N_3O_2$, Mol. Wt. 241.25, Calculated C:64.69, H:4.56, N:17.42 Found C:64.65, H:4.53, N:17.38; The FTIR in (KBr cm^{-1}) : 3861 (N-H stretching), 3162 (C-OH), 1622 (C=O), 16079 (aliphatic C=N), 1389 (aromatic C=N), 1554 (Ar, C=C) (Figure S13). ^{1}H NMR (400 MHz, DMSO *d*$_6$) δ 12.26 (s, 1H, D_2O exchangeable NH), 11.15 (s, 1H OH), 8.63 (s, 1H, aliphatic), 8.759-8.751 (d, 2H, J=3.2 Hz, Pry-H), 7.834-7.830 (d, 2H, J= 1.6 Hz, Ar-H), 7.520-7.516, (d, 2H, J=6 Hz, Pry-H), .501-7.497 (t, 2H, J =1.6 Hz, Ar-H);) (Figure S14). ^{13} C NMR (100 MHz, DMSO *d*$_6$): 116.86, 118.83, 121.87, 130.03, 132.01, 140.28, 149.94, 150.66, 158.06, 161.72ppm (Figure S15). The UV–Visible absorbance peaks was shifted to a longer wavelength (lower frequency) observed at 317 nm(Figure S16).

N-[(E)-(4-Hydroxyphenyl)methylene]isonicotinohydrazide (3e)-Yield: 95 %, MP: 285-287^{o}C; elemental analysis: molecular formula: $C_{13}H_{11}N_3O_2$, Mol. Wt. 241.25, Calculated C:64.69, H:4.56, N:17.42 Found C:64.65, H:4.53, N:17.38; The FTIR in (KBr cm^{-1}) : 3502-

3628 (N-H stretching), 3161 (C-OH), 1652 (C=O), 1683 (C=N), 1552 (Ar, C=C), 1363 (Ar, C=N) (Figure S17). ^{1}H NMR (400 MHz, DMSO d_6) δ 11.78 (s, 1H, D_2O exchangeable NH), 9.7 (s, 1H, OH), 8.33 (s, 1H, aliphatic), 8.68-8.67 (d, 2H, J=6.4 Hz, Pry-H), 7.786-7.782 (d, 2H, J=1.6 Hz, Ar-H), 7.54-7.52 (d, 2H, J=8.4 Hz, Pry-H), 6.80-6.77 (d, 2H, J=8.8 Hz, Ar-H) (Figure S18). ^{13}C NMR (100 MHz, DMSO d_6): 116.03, 121.84, 125.28, 129.44, 141.01, 149.62, 149.98, 150.42, 160.15, 161.86 ppm(Figure S19). The UV–Visible absorbance peaks was shifted to a longer wavelength (lower frequency) observed at 317 nm(Figure S20).

2.1.3. Experimental protocol for antimicrobial activity of Schiff bases.

Prepared INZ incorporated Schiff base (3a-e) (Scheme 1) was performed *in vitro* against bacterial strains *viz.* (*gram-positive* and *gram negative*) and fungi respectively, Minimum inhibition zone (mm) values for bacteria were determined according to the twofold broth microdilution method using Muller-Hinton broth in 96-well micro test plates recommended by National Committee for Clinical Laboratory Standards (NCCLS) guidelines. Dimethylsulfoxide (DMSO) was used as solvent control. Tetracycline was used as a standard antibacterial drug, and Nystatin was used as a standard antifungal drug for reference. The plates were incubated at 37^{o}C for all microorganisms; absorbance at 595 nm was recorded to assess the inhibition zone of cell growth after 24 h. The compounds (Scheme 2) showing moderate to significant antibacterial activity were selected for minimum inhibitory concentration studies.

2.1.4. Formation of complexes from biologically active Schiff bases with Ce^{+3} metal ion.

Medicinally active INZ incorporated Schiff base (3a-e) (Scheme 1) was used for metal complexation (4a-e) (Scheme 3). They are easily donating lone pairs from atom to metal ion at the time of complexation. We have used a freshly prepared Schiff base (organic ligand) (Scheme 1) solution at the time of each complexation to reduce the percentage of degradation of ligands. The stability constant of prepared complexes was checked by the pH-metric method. They afford several benefits, such as being easily handled, accuracy, and robustness. All solutions were prepared by double distilled water (pH- 6.80-6.40) and potassium permanent solution.

2.1.5. Complexation procedure.

Metal salt[$Ce(NO_3)_3.6H_2O$] with N-[(E)-(4-(R)methylene] isonicotinohydrazide (organic ligand) (Scheme 1) by using mixed ethanol (70%) and water (30%) solvent. Prepared solution of Ce^{+3} metal salt [$Ce(NO_3)_3.6H_2O$] with N-[(E)-(4-(R)methylene] isonicotinohydrazide (organic Ligands) mixed homogenously.

An aqueous solution of NH_4OH (alkali) was used to maintain the solution of *pH*. The mixed solution was refluxed for 4 to 5 hours and obtained color precipitate (Scheme 3). The colored residue was cooled at room temperature, filtered with Whatman filter paper no. 41, dried & weight.

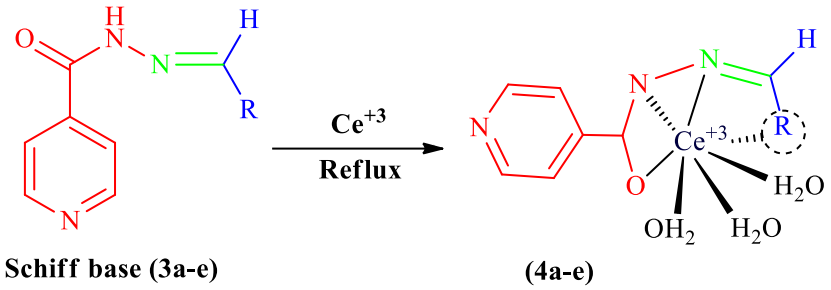

Scheme 3. Synthesized Ce^{+3} Metal complex with INZ Schiff bases.

2.1.6. Determination of stability constant by potentiometry.

In the present study, stability constants of the prepared complex (Scheme 3) have been determined by Calvin-Bjerrun. pH metric titration of solutions- experimental procedure.

$HClO_4$

$HClO_4$ + Ligand (A + L)

$HClO_4$ + Ligand + Metal ion (A+ L+ M)

Ligand solutions (0.01 M) were prepared by dissolving the requisite amount of ligand in 7:3 ratio of ethanol and distilled water. Ce^{+3} metal ion solution was prepared and standardized by EDTA solution. pH metric titrations were recorded on Elico-Digital pH -meter (Model no L-120) at specific temperatures. The pH meter was standardized by 4, 7 & 9.2 pH buffer solutions. The complex solution was prepared in 50 ml quantity and titrated with standardized 0.2 N NaOH solution by using combined glass-calomel electrode pH-meter and noted constant pH reading at three systems.

(A) 0.2 N $HClO_4$ (5 ml) + 1 M $NaClO_4$ (5ml)

(A + L) 0.2 N $HClO_4$ (5ml) + 0.01 N ligand (10ml)

(A + L + M) 0.2 N $HClO_4$ (5ml) + 0.01 N ligand (10ml) + 0.01M Ce^{+3} metal ion solution (10 ml).

The pH of hydrolysis of metal ions was observed by titration of metal ion solution in $HClO_4$ at 1M $NaClO_4$ ionic strength in the presence of ligand. The graphical representation was made between pH and volume of alkali added (NaOH). These values were utilized for the calculation of $\overline{n_A}$, $\bar{n}$ and pL. The proton-ligand formation number $\overline{n_A}$ Defined as hydrogen ions bound to one ligand molecule, it was calculated using the formula (1).

$$\bar{n}_A = \gamma - \left[\frac{(\varepsilon^0+N)\times(V_2-V_1)}{(V_0-V_1)\times T_L^0}\right] \quad \text{.....(1)}$$

Where γ denote the replaceable H^+ ion, ε^0 is ca concentration of acid, T_L^0 is concentration of ligand, N is normality of alkali, V_1 and V_2 are the volumes of alkali required during the acid and ligand titrations at the given pH and V_0 is the total volume of the mixture. The average number $\bar{n}$ of Ce^{+3} metal ions associated with the ligand at different pH values was calculated from the metal ions and ligand titration curves using equation (2).

$$\bar{n} = \left[\frac{(E^0+N)\times(V_3-V_2)}{(V_0+V_2)\times T_m^0}\right] \quad \text{..... (2)}$$

Where N, E^0, V_0, and V_2 have the same significance as in Eq. (1), V_3 is the volume of alkali added in the metal titration to attain the given pH reading, and T^0m is the concentration of the metal ion present in solution and $\bar{n}$ Is the average number of protons- ligand stability constant. The free ligand concentration was calculated by the following expression (3).

$$pL = \log\left[\frac{1+\frac{H+}{K}}{T_L^0-T_M^0\,\bar{n}} \times \frac{V_0+V_3}{V_0}\right] \quad \text{.....(3)}$$

T_L^0 and T_M^0 are the stoichiometric concentration of the ligand and the metal ions, respectively, V_0 Is the initial volume of the solution and V_3 is volume at a particular pH in (A+R+M) titration. The approximate peak value was calculated by the formula (4).

$$\text{Log } \frac{\bar{n}_A - 1}{1 - \bar{n}_A} = pK - pH \quad \ldots\ldots\ldots\ldots\ldots\ldots\ldots\ldots\ldots\ldots(4)$$

The pK values were obtained from the formation curves and a point-wise calculation. The metal-ligand stability constant, i.e., calculation logic by formula (5).

$$\text{Log } \frac{\bar{n}}{1 - \bar{n}} = \text{logK} - \text{pL} \quad \ldots\ldots\ldots\ldots\ldots\ldots\ldots\ldots\ldots\ldots(5)$$

The values of log k were determined by using the value of $\bar{n}$ in the range of 0.2 to 0.8. The standard solution of sodium hydroxide is used to titration against acid, acid + ligand mixture, and acid + ligand + metal ion solution by Potentiometrically. The results are shown in table 1-5.

3. Results and Discussion

3.1. Antibacterial & antifungal activity.

The minimum inhibition zone (mm) for 3a, 3b, 3c, 3d, and 3e Schiff base was determined against gram-positive bacteria *(B. subtilis, B.megaterium, S.aureus, B.cereus)* and gram-negative bacteria *(E.Coli, S.boydii, S.abony, P. aerogenosa, E. aerogenes, S. typhi* (Table 1) and fungi *(C. albicans, S. cerevisiae, A. niger)* (Table 2).

Table 1. *In vitro* antibacterial evaluation for synthesized Schiff base derivatives(3a-e) in Minimum inhibition zone (mm) against *Gram +ve & Gram -ve* bacterial stains.

Antibacterial activity with gram +ve & -ve bacterial stains
Minimum inhibition zone (mm)

Bacterial Stain ↓	**Schiff Base →**	**(3a)**	**(3b)**	**(3c)**	**(3d)**	**(3e)**	**Teracyclin**
B. subtilis (Gram +ve)		12	9	8	14	15	34
B. megaterium (Gram +ve)		-	-	-	-	-	32
S. aureus (Gram +ve)		14	10	-	25	13	34
B. cereus (Gram +ve)		9	12	-	-	16	33
S. typhi (Gram -ve)		-	9	10	8	-	31
E. aerogenes (Gram -ve)		-	5	-	11	-	33
P. aerogenosa (Gram -ve)		-	-	-	14	14	30
S. abony (Gram -ve)		-	-	-	12	-	30
E. coli (Gram -ve)		12	6	10	16	9	34
S. boydii (Gram -ve)		6	-	-	12	-	30

Table 2. *In vitro* antifungal evaluation of synthesized Schiff base derivatives(3a-e) in Minimum inhibition zone (mm) against *fungi.*

Antifungal activity- *Minimum inhibition zone (mm)*

Fungi ↓	**Schiff Base →**	**(3a)**	**(3b)**	**(3c)**	**(3d)**	**(3e)**	**Nystatin**
C. albicans		-	-	8	11	10	30
S. cerevisiae		-	-	6	14	-	29
A. niger		-	-	8	18	16	30

All Schiff bases (3a-e) showed moderate to significant activity against gram-positive & gram-negative bacterial stains. All Schiff bases (3a-e) active against *B. Subtilis* gram-positive & *E. Coli* gram-negative bacterial stains. In the case of fungi, Schiff base (3c), (3d), (3e) showed good activity against *C. Albicans, S. Cerevisiae & A. Niger* fungi.

3.2. Complexation of Ce^{+3} metals with ligand (3a-e).

Parameters: N = 0.2, T_M^0= 0.002, T_L^0= 0.002, V_0 = 50 ml, γ=1, ε^0 = 0.02 & T = 27 ± 1.

Table 3. Potentiometrically titration data for compounds (4a-e).

Vol. of Alkali Added	pH						
	Acid	Acid+ Ligand	A + L(a-e) + Ce^{+3}				
			4a	4b	4c	4d	4e
0.6	2.15	2.17	2.09	2.06	2.07	2.08	2.05
1.2	2.27	2.23	2.19	2.12	2.15	2.15	2.12
1.8	2.41	2.39	2.31	2.20	2.23	2.29	2.24
2.4	2.63	2.50	2.48	2.27	2.35	2.41	2.37
3	3.07	2.80	1.71	2.43	2.53	2.54	2.49
3.6	10.62	3.95	3.17	2.59	2.88	2.75	2.89
4.2	11.14	7.95	4.71	3.02	3.42	3.51	6.88
4.8	11.32	9.90	6.98	3.43	6.60	7.53	7.49
5.4	11.42	10.18	7.89	6.87	7.18	8.45	8.31
6	11.51	10.70	8.92	8.38	7.85	9.19	9.28
6.6	11.59	10.84	8.41	9.35	8.41	9.48	9.77
7.4	11.66	11.11	10.18	10.25	9.15	10.03	10.13
8	11.71	11.25	10.48	10.59	9.72	10.20	10.25

Table 4. Protonation constant of (4a-e).

pH	V_1	V_2	$\Delta V = V_2 - V_1$	$\bar{n}_A$	pK
Compound (4a)					
2.2	0.85	1	0.15	0.6755162	2.518442797
2.4	1.76	2	024	0.4899536	2.38254321
2.6	2.32	2.725	0.405	0.1485092	1.84157331
2.8	2.67	3	0.33	0.31080031	2.454142054
3	2.92	3.125	0.205	0.5738851	3.129298246
3.2	3.0741	3.224	0.1499	0.6893212	3.546109928
3.4	3.1881	3.284	0.0959	0.8016662	4.006596737
3.6	3.2059	3.344	0.1386	0.7134501	3.996163424
3.8	3.2114	3.424	0.2126	0.5605077	3.905630332
4	3.2174	3.6035	0.3861	0.201934	3.403170515
4.2	3.2234	3.6175	0.3941	0.1854898	3.557423623
4.4	3.2294	3.6315	0.4021	0.1690494	3.708438536
Compound (4b)					
2.2	0.85	1.067	0.217	0.53058014	2.253189526
2.4	1.76	2.03334	0.27334	0.41909969	2.258215733
2.6	2.32	2.775	0.455	0.04338685	1.256621775
2.8	2.67	3.03705	0.36705	0.2334251	2.283592958
3	2.92	3.18525	0.26525	0.4486489	2.910478369
3.2	3.0741	3.252938	0.178838	0.62934501	3.429918942
3.4	3.1881	3.311758	0.123658	0.74425896	3.863923645
3.6	3.2054	3.370578	0.165178	0.6585012	3.885167398
3.8	3.2114	3.4953	0.2839	0.41311448	3.647517029
4	3.2174	3.60711	0.38971	0.19447211	3.382776741
4.2	3.2234	3.62291	0.39951	0.17430867	3.524501261
4.4	3.2294	3.63871	0.40931	0.15414977	3.660649424
Compound (4c)					
2.2	0.85	0.8	-0.05	1.10816126	3.210531231
2.4	1.76	1.8	0.04	0.91499227	3.431959017
2.6	2.32	2.6892	0.3692	0.22377676	2.059828336
2.8	2.67	2.97655	0.30655	0.35977786	2.54970375
3	2.92	3.1125	0.1925	0.59986772	3.175851912
3.2	3.0741	3.21968	0.14558	0.69827468	3.56441453
3.4	3.1881	3.28528	0.09718	0.79901895	3.999401978
3.6	3.2054	3.35088	0.14548	0.69922602	3.966377315
3.8	3.2114	3.4455	0.2341	0.51606235	3.82791276
4	3.2174	3.602373	0.384973	0.20426346	3.40942137
4.2	3.2234	3.618193	0.394793	0.18405758	3.553294184
4.4	3.2294	3.634013	0.404613	0.16385625	3.692182071
Compound (4d)					
2.2	0.85	1	0.15	0.675516224	12.4092579
2.4	1.76	2.0334	0.2734	0.418972179	2.257988258
2.6	2.32	2.8	0.48	0.009174312	0.558607315
2.8	2.67	3.0244	0.3544	0.259844314	2.345390137
3	2.92	3.1464	0.2264	0.529402872	3.026860396
3.2	3.0741	3.2341	0.16	0.668388159	3.504398718
3.4	3.1881	3.2961	0.108	0.776641768	3.941218779

pH	V_1	V_2	$\Delta V = V_2 - V_1$	$\bar{n}_A$	pK
3.6	3.2054	3.3581	0.1527	0.684298962	3.935969872
3.8	3.2114	3.46672	0.25532	0.472195808	3.751649291
4	3.2174	3.606256	0.388856	0.196237321	3.387653769
4.2	3.2234	3.621896	0.398496	0.176404363	3.530795287
4.4	3.2294	3.637536	0.408136	0.156575877	3.668678835
Compound (4e)					
2.2	0.85	1	0.15	0.67551622	2.5184428
2.4	1.76	1.88	0.12	0.74497682	2.86556309
2.6	2.32	2.76	0.44	0.07492355	1.50844071
2.8	2.67	3.019356	0.349356	0.27037858	2.36887472
3	2.92	3.148396	0.228396	0.52525397	3.043908
3.2	3.0741	3.23876	0.16466	0.65872996	3.50560558
3.4	3.1881	3.30336	0.11526	0.76162713	3.90448558
3.6	3.2054	3.36796	0.16256	0.66391381	3.89566104
3.8	3.2114	3.5053	0.2939	0.39244222	3.61018814
4	3.2174	3.60847	0.39107	0.191661	3.37494021
4.2	3.2234	3.62387	0.40047	0.17232458	3.51848717
4.4	3.2294	3.63927	0.40987	0.15299252	3.65678295

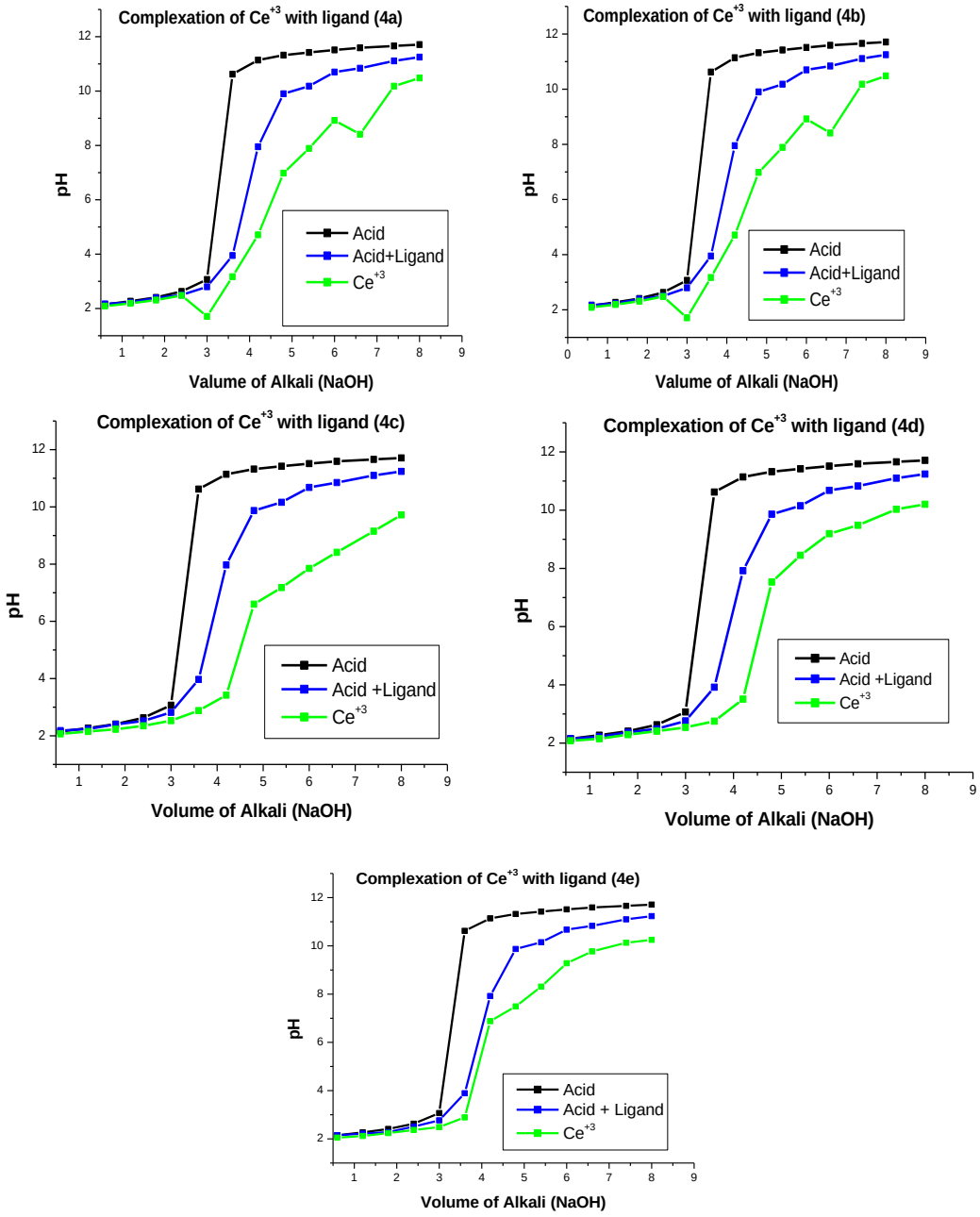

Figure 1. pH metric titration curves of complexation of Ce^{+3} metal with ligands (3a-e).

Table 5. Metal-Ligand Stability Constant of Ce^{+3} metal with Ligands (3a-e).

Ligand	pK	Stability Constant (logK)
(3a)	4.59	3.9004
(3b)	3.59	3.5275
(3c)	3.56	3.2665
(3d)	3.78	4.0212
(3e)	3.73	4.4984

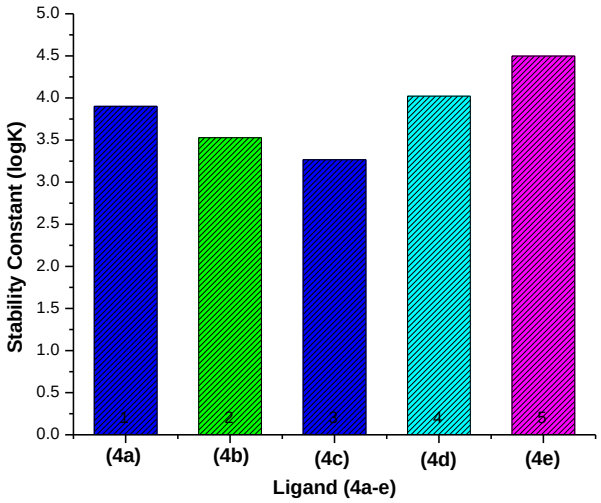

Figure 2. Stability constant of Ce^{+3} metals with ligand (3a-e) complexes (4a-e).

All complexes (4a-e) (Scheme 3). have been successfully carried out potentiometrically; the pH metric titration curve (Figure 1) has indicated the complex formation. Complex Ce^{+3} metal ions with ligand (3e) showed higher stability than other Ce^{+3} ligand complexes. The order of stability constant of Ce^{+3} complexes is (3e) > (3d) > (3a) > (3b) > (3c) shows in (Table 5 & Figure 2).

4. Conclusions

In the present study, we successfully synthesized bio-active organic ligands (3a-e) (Scheme 2) and their complexation (Scheme 3) with the inner transition element (Ce^{+3}). Synthesized ligands (3a-e) (Scheme 2) have been confirmed by various spectroscopic techniques and studied for their *in vitro* antibacterial and antifungal activity. All ligands (3a-e) (Scheme 2) showed moderate to significant antibacterial as well as antifungal activity. Complexation of synthesized Bio-active Schiff bases (3a-e) (Scheme 2) has been successfully developed with Ce^{+3} metal ions potentiometrically, which may be helpful to improve stability of bio-active organic ligands. The order of stability constants of ligands with Ce^{+3} metal ions is found as (3e) > (3d) > (3a) > (3b) > (3c).

Funding

This research received no external funding.

Acknowledgments

The authors are grateful to Principal Dr. Rafiq Zakaria College for Women Aurangabad, (MS) India providing the necessary facilities.

Conflicts of Interest

The authors declare no conflict of interest.

References

1. Durgun, M.; Turkeş, C.; Işık, M.; Demir, Y.; Sakli, A.; Kuru, A.; Güzel, A.; Beydemir, S.; Akocak, S.; Osman, S.M.; AlOthman, Z.; Supuran, C. T. Synthesis, characterisation, biological evaluation and in silico studies of sulphonamide Schiff bases. *Journal of Enzyme Inhibition and Medicinal Chemistry* **2020,** *35*, 950–962, doi:10.1080/14756366.2020.1746784.
2. Turkeş, C.; Beydemir, S. Inhibition of Human Serum Paraoxonase-I with Antimycotic Drugs: In Vitro and In Silico Studies. *Appl Biochem Biotechnol* **2020**, *190*, 252–269, https://doi.org/10.1007/s12010-019-03073-3.
3. Naureen, B.; Miana, G.A.; Shahid, K.; Asghar, M.; Tanveer, S.; Sarwar, A. Iron (III) and zinc (II) monodentate Schiff base metal complexes: Synthesis, characterisation and biological activities. *Journal of Molecular Structure*, **2021,** *1231*, 129946, doi:10.1016/j.molstruc.2021.12994.
4. Arora, A.; Sharma, R.; Tageza, A.; Grewal, A.S.; Saini, B.; Arora, S.; Kau, R. Design and synthesis of novel 4-aminophenazone Schiff bases by grinding technique as prospective anti-inflammatory agents, *Journal of Applied Pharmaceutical Science* **2021**, *11* (Supp 1), 048-053, DOI: 10.7324/JAPS.2021.11s105.
5. Kaya, I.; Daban, S.; Senol, D. Synthesis and characterization of Schiff base, Co(II) and Cu(II) metal complexes and poly(phenoxy-imine)s containing pyridine unit. *Inorganica Chimica Acta* **2021**, *515*, 120040. doi:10.1016/j.ica.2020.120040.
6. Sumrra, S. H.; Zafar, W.; Asghar, M. L.; Mushtaq, F.; Raza, M. A.; Nazar, M. F.; Nadeem, M.A.; Imran, M.; Mumtaz, S. Computational investigation of molecular structures, spectroscopic properties, cholinesterase inhibition and antibacterial activities of triazole Schiff bases endowed metal chelates. *Journal of Molecular Structure* **2021**, *1238*, 130382. doi:10.1016/j.molstruc.2021.130382.
7. Gur, M.; Yerlikaya, S.; Sener, N.; Ozkınalı, S.; Baloglu, M. C.; Gokce, H.; Altunoglu, Y.C.; Demir, S.; Sener, I. Antiproliferative-antimicrobial properties and structural analysis of newly synthesized Schiff bases derived from some 1,3,4-thiadiazole compounds. *Journal of Molecular Structure* **2020**, *1219*, 128570. doi:10.1016/j.molstruc.2020.12857.
8. Catalano, A.; Sinicropi, M. S.; Iacopetta, D.; Ceramella, J.; Mariconda, A.; Rosano, C.;Scali, E.; Saturnino, C.; Longo, P. A Review on the Advancements in the Field of Metal Complexes with Schiff Bases as Antiproliferative Agents. *Applied Sciences* **2021**, *11*, 6027. doi:10.3390/app11136027.
9. Uddin, M. N.; Ahmed, S. S.; Alam, S. M. R. REVIEW: Biomedical applications of Schiff base metal complexes. *Journal of Coordination Chemistry* **2020**, *73*, 3109–3149. doi:10.1080/00958972.2020.1854745.
10. Irfan, R. M.; Shaheen, M. A.; Saleem, M.; Tahir, M. N.; Munawar, K. S.; Ahmad, S.; Rubab, S.L.; Tehreem Tahirf, T.; Mojzych K.K; Mojzych, M. (2021). Synthesis of new cadmium(II) complexes of Schiff bases as alkaline phosphatase inhibitors and their antimicrobial activity. *Arabian Journal of Chemistry* **2021**, *14*, 103308. doi:10.1016/j.arabjc.2021.103308.
11. Peng, D.-L. Syntheses, characterization and crystal structures of Schiff base nickel(II) complexes with antibacterial activity. *Inorganic and Nano-Metal Chemistry* **2018**, *48*, 530-534, https://doi.org/10.1080/24701556.2019.1567540.
12. Baglia, R.A.; Zaragoza, J.P.T.; Goldberg, D.P. Biomimetic Reactivity of Oxygen-Derived Manganese and Iron Porphyrinoid Complexes. *Chemical Reviews* **2017**, *117*, 13320-13352, https://doi.org/10.1021/acs.chemrev.7b00180.
13. Sherman, S.E.; Xiao, Q.; Percec, V. Mimicking Complex Biological Membranes and Their Programmable Glycan Ligands with Dendrimersomes and Glycodendrimersomes. *Chemical Reviews* **2017**, *117*, 6538-6631, https://doi.org/10.1021/acs.chemrev.7b00097.
14. Jasniewski, A.J.; Que, L. Dioxygen Activation by Nonheme Diiron Enzymes: Diverse Dioxygen Adducts, High-Valent Intermediates, and Related Model Complexes. *Chemical Reviews* **2018**, *118*, 2554-2592, https://doi.org/10.1021/acs.chemrev.7b00457.
15. Mahmoud, W.H.; Deghadi, R.G.; Mohamed, G.G. Metal complexes of novel Schiff base derived from iron sandwiched organometallic and 4-nitro-1,2-phenylenediamine: Synthesis, characterization, DFT studies, antimicrobial activities and molecular docking. *Applied Organometallic Chemistry* **2018**, *32*, https://doi.org/10.1002/aoc.4289.
16. Anar, M.; Özkan, E.H.; Öğütçü, H.; Ağar, G.; Şakıyan, İ.; Sarı, N. Useful agents against aflatoxin B1 – antibacterial azomethine and Mn(III) complexes involving L-Threonine, L-Serine, and L-Tyrosine. *Artificial*

Cells, Nanomedicine, and Biotechnology **2016**, *44*, 853-858, https://doi.org/10.3109/21691401.2014.991792.
17. Logoglu, E.; Koyuncu, E.A.; Karaboga, M.N.S.; Sari, N. Synthesis and a suggestion mechanism on biological evaluation of Amino Acid-Schiff base ligands and Co(II), Cu(II) and Ni(II) Complexes. *Gazi University Journal of Science* **2016**, *29*, 303- 307.
18. Chakraborty, H.; Paul, N.; Rahman, M.L. Catalytic activity of Schiff base aquocomplexes of copper (II) towards hydrolysis of amino acid esters. *Trans. Met. Chem*. **1994,** *19*, 524-526, https://doi.org/10.1007/BF00136366.
19. Xi, Z.; Liu, W.; Cao, G.; Du, W.; Huang, J.; Cai, K.; Guo, H. Catalytic oxidation of naphthol by metalloporphyrin's, Cuihau Xuebao. *Chem. Abstr*. **1987**, *106*.
20. Selvaraj K.; Theivarasu, C. Synthesis and Characterization of Samarium(Iii) Complexes with Piperidin-4-Ones. Synthesis and Reactivity in Inorganic and Metal-Organic Chemistry, *Synth. React. Inorg. Met-Org. Chem*. **2000,** *30*, 1113-1128, https://doi.org/10.1080/00945710009351823.
21. Kostova, I.; Momekov, G.; Stancheva, P. New Samarium(III), Gadolinium(III), and Dysprosium(III) Complexes of Coumarin-3-Carboxylic Acid as Antiproliferative Agents. *Metal-Based Drugs* **2007**, 1–8, https://doi.org/10.1155/2007/15925.
22. Mumtaz, A.; Mahmud, T.; Elsegood, M.R.; Weaver, G.W. Synthesis and characterization of new Schiff base transition metal complexes derived from drug together with biological potential study. *J Nucl Med Radiat Ther* **2016**, *7*, https://doi.org/10.4172/2155-9619.1000310.
23. Mishra, A.P.; Soni, M. Synthesis, Structural, and Biological Studies of Some Schiff Bases and Their Metal Complexes. *Metal-Based Drugs* **2008**, *2008*, https://doi.org/10.1155/2008/875410.
24. Zamzam, T.; Jadhav, S.; Kayande, D.; Megha, R. pH-metric Study of Metal-ligand Stability Constant of Transition Metal Complexes with Pharmacologically Active Ligand N-[(E)-(4-Hydroxy-3-methoxyphenyl)methylene] isonicotinohydrazide. *Curr. Pharm. Res*. **2019,** *407*, 58-65.
25. Zamzam, T.; Jadhav, S.; Farooqui, M.; Megha, R. Stability constant study of transition metal complexes with pharmacologically active ligand(N-[-(4- chlorophenyl)methylene] nicotinohydrazide) by pH metric Technique. *Int. J. Chem. Tech. Res.* **2018,** *11*, 211-216, https://doi.org/10.20902/IJCTR.2018.111121.
26. Zamzam, T.; Jadhav, S.; Megha, R. Potentiometric and Thermodynamic Studies of (N- [-(4-Chlorophenyl) Methylene]Nicotinohydrazide) and Its Transition Metal Complexes. *Integr. Ferroelectric*. **2020,** *205*, 88-94, https://doi.org/10.1080/10584587.2019.1675003.
27. Zamzam, T.; Jadhav, S.; Farooqui, M.; Megha, R. Determination of Metal-Ligand Stability Constant of Transition Metal Complexes with Pharmacologically Active Ligand N-[(E)-(2-Nitrophenyl)methylen]isonicotinohydrazid. *J. Biol. Chem. Chron.* **2019**, *5* 91-95, http://dx.doi.org/10.33980/jbcc.2019.v05i01.015.

Supplementary Data

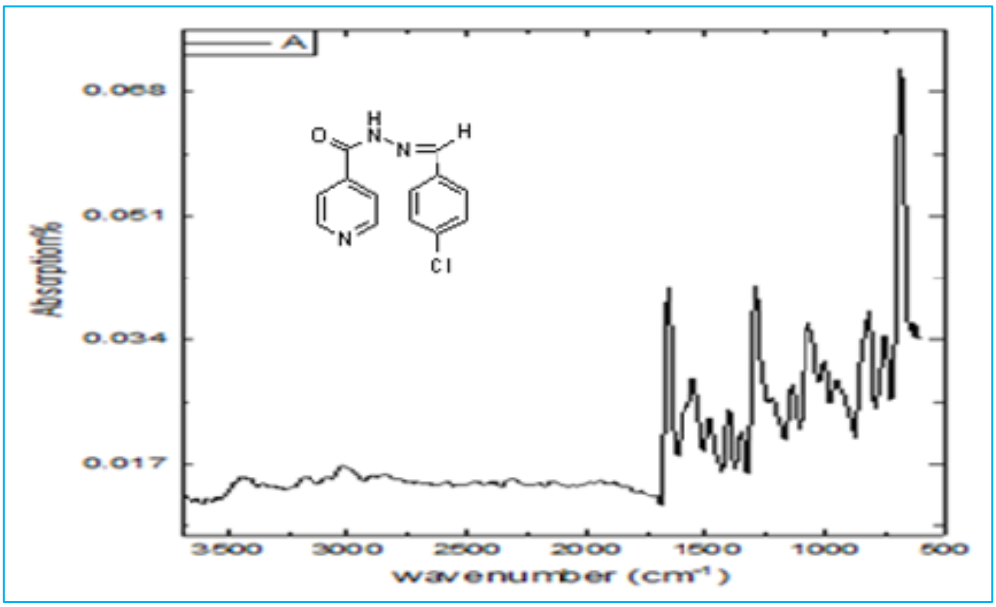

Figure S1. FT-IR spectra of N-[(E)-(4-chlorophenyl) methylene] isonicotinohydrazide (3a).

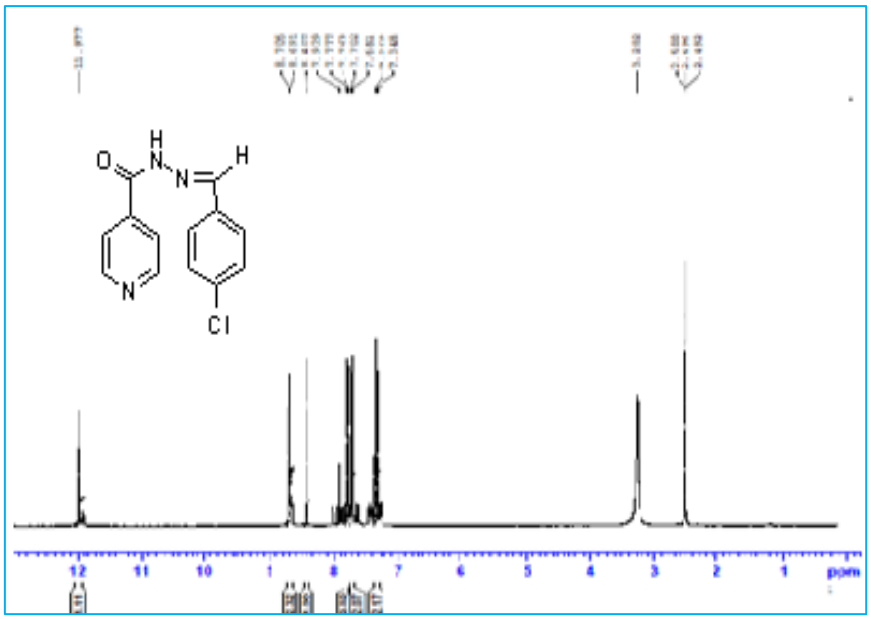

Figure S2. ^{1}H NMR spectroscopy of N-[-(4-chlorophenyl) methylene]isonicotinohydrazide (3a).

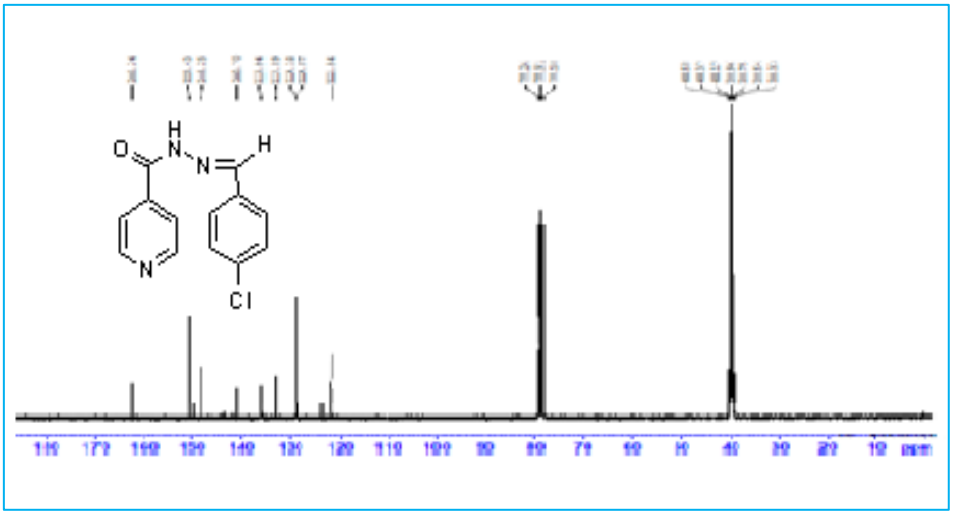

Figure S3. ^{13}CNMR spectroscopy of N-[-(4-chlorophenyl) methylene]isonicotinohydrazide (3a).

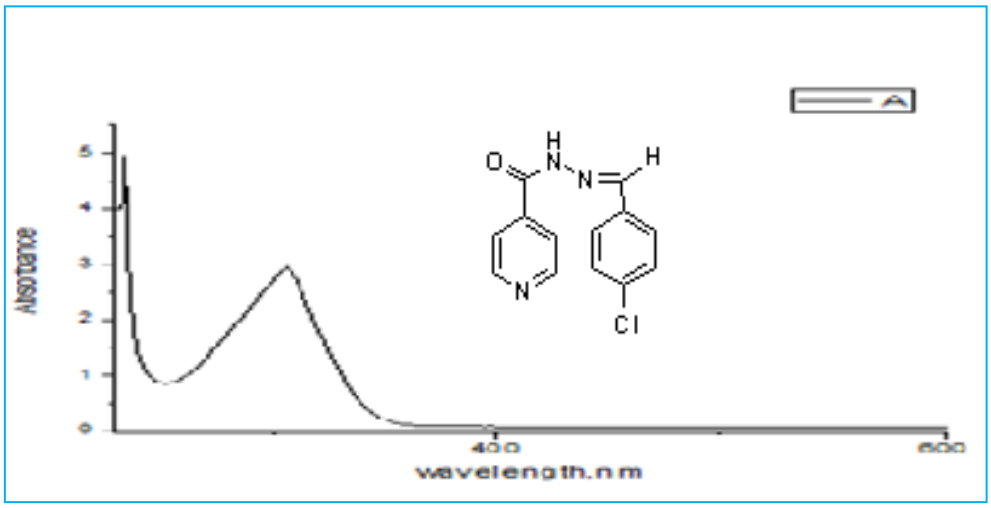

Figure S4. UV–Vis spectroscopy of N-[-(4-chlorophenyl) methylene]isonicotinohydrazide (3a).

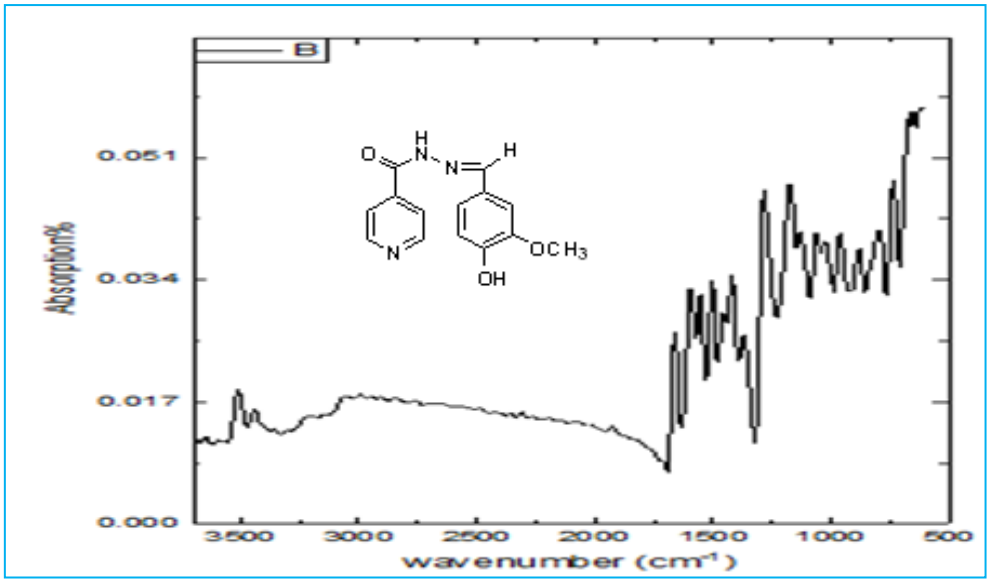

Figure S5. FT-IR spectra of N-[(E)-(4-Hydroxy-3-methoxyphenyl) methylene]isonicotinohydrazide (3b).

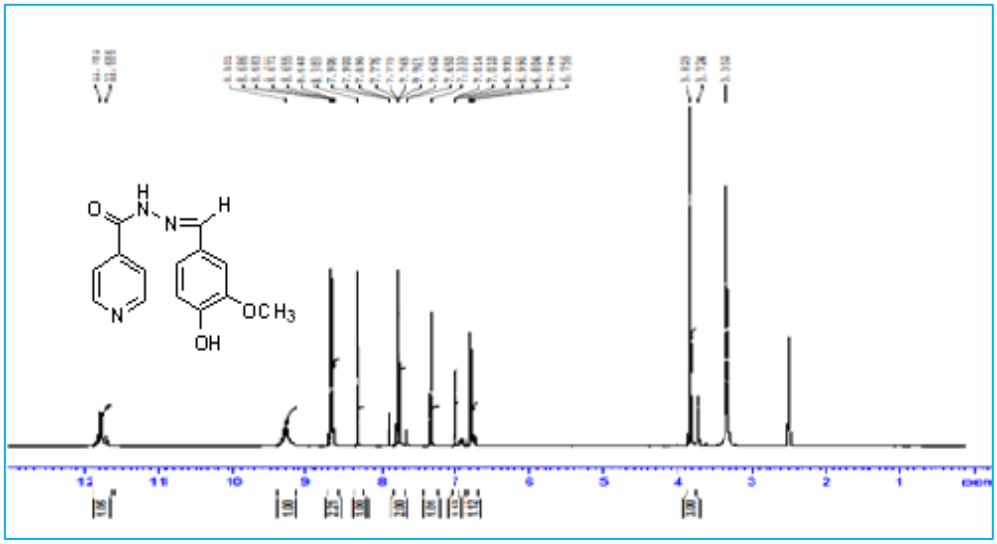

Figure S6. [1]H NMR of N-[(E)-(4-Hydroxy-3-methoxyphenyl) methylene] isonicotinohydrazide (3b).

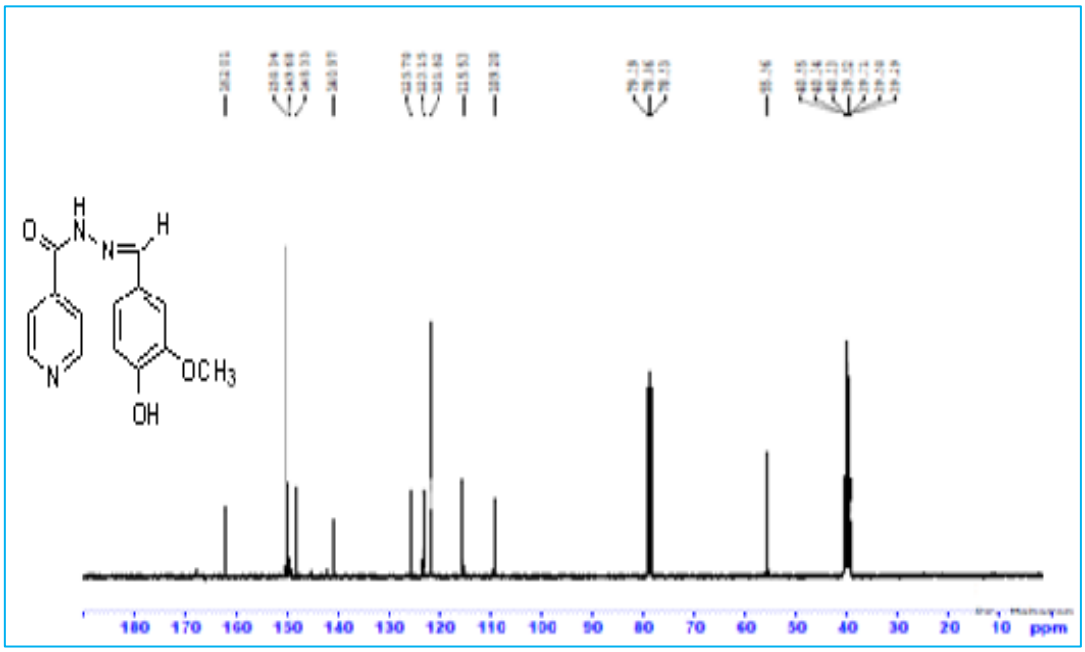

Figure S7. ^{13}CNMR of N-[(E)-(4-Hydroxy-3-methoxyphenyl) methylene]isonicotinohydrazide (3b).

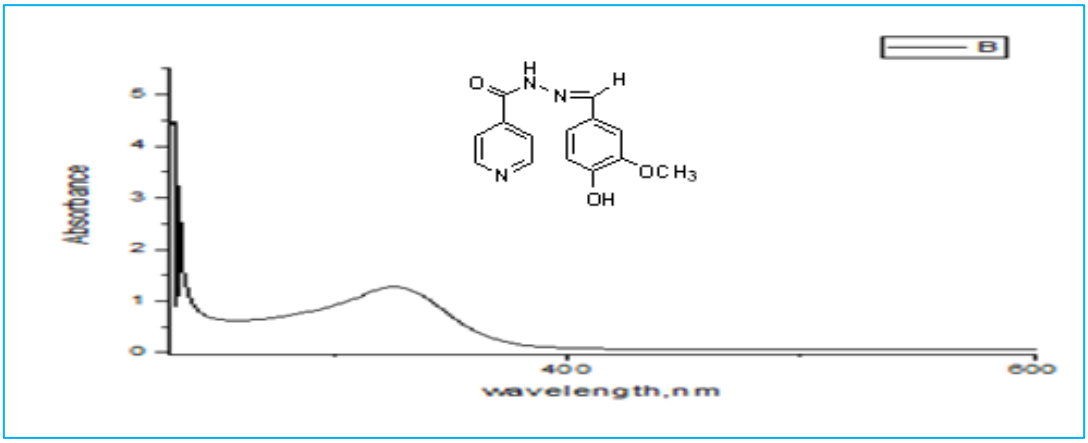

Figure S8. UV–Vis spectra of N-[(E)-(4-Hydroxy-3-methoxyphenyl) methylene] isonicotinohydrazide (3b).

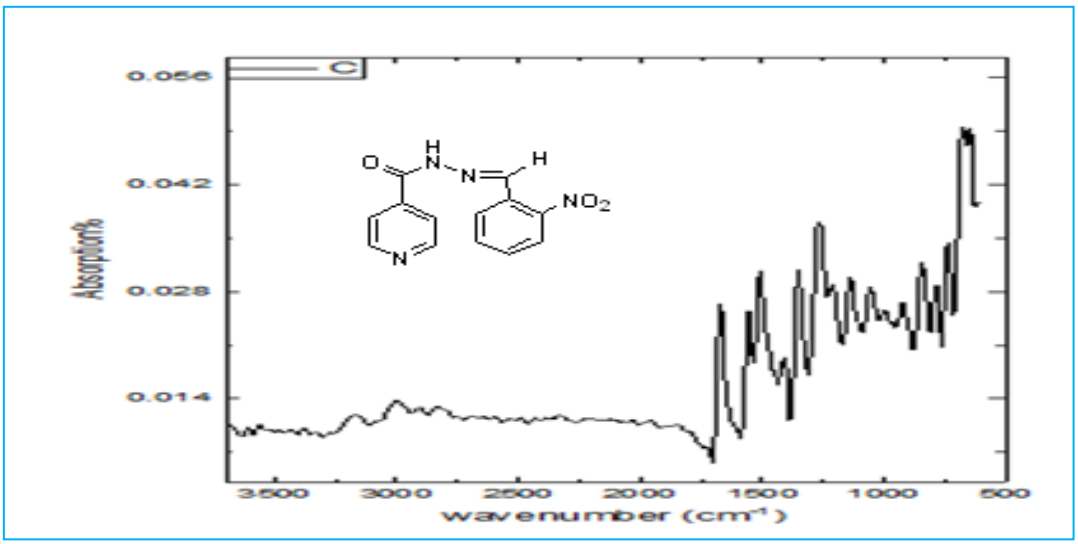

Figure S9. FT-IR spectra of N-[(E)-(2-Nitrophenyl) methylene] isonicotinohydrazide (3c).

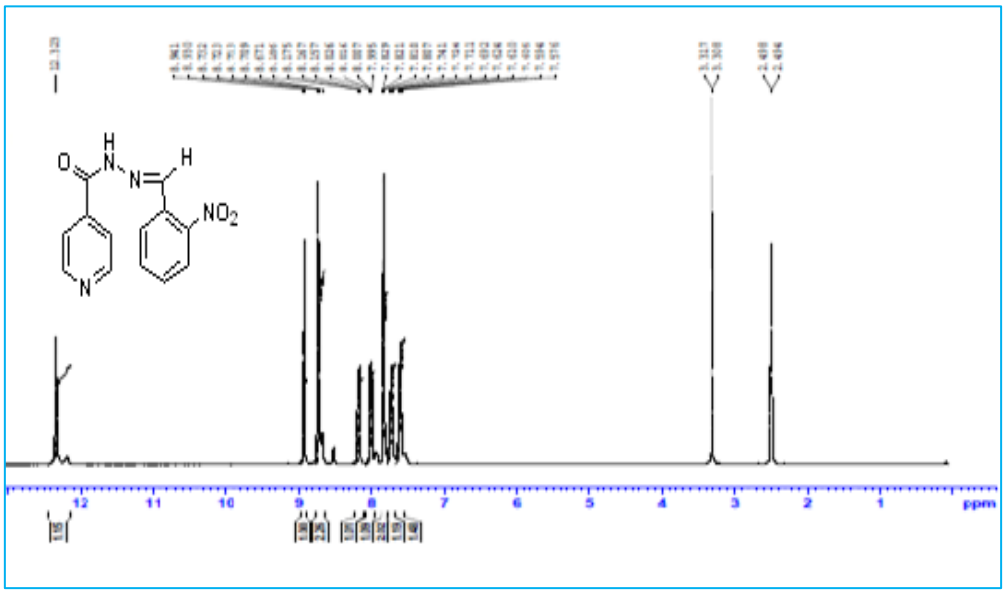

Figure S10. ^{1}H NMR of N-[(E)-(2-Nitrophenyl) methylene] isonicotinohydrazide(3c).

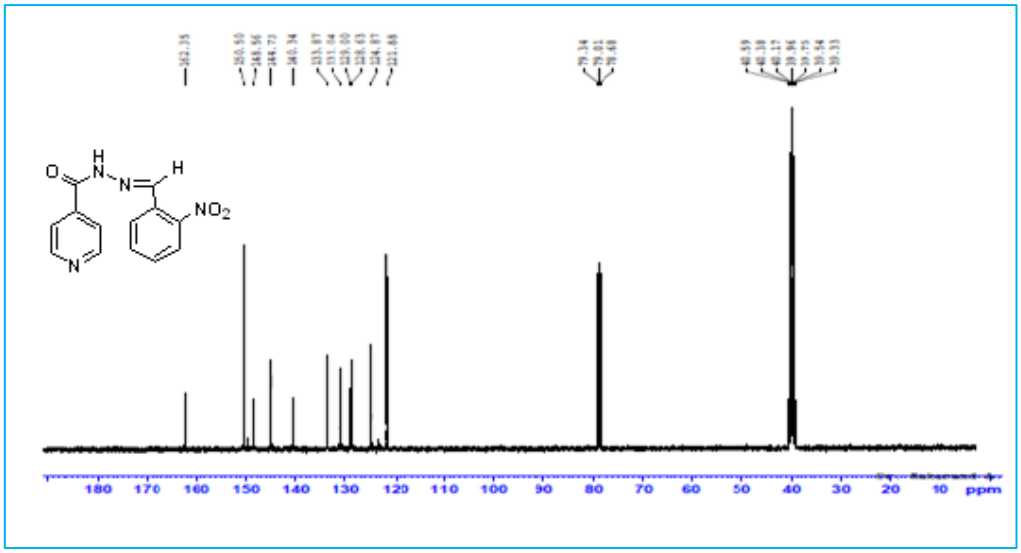

Figure S11. ^{13}CNMR of N-[(E)-(2-Nitrophenyl) methylen] isonicotinohydrazide(3c).

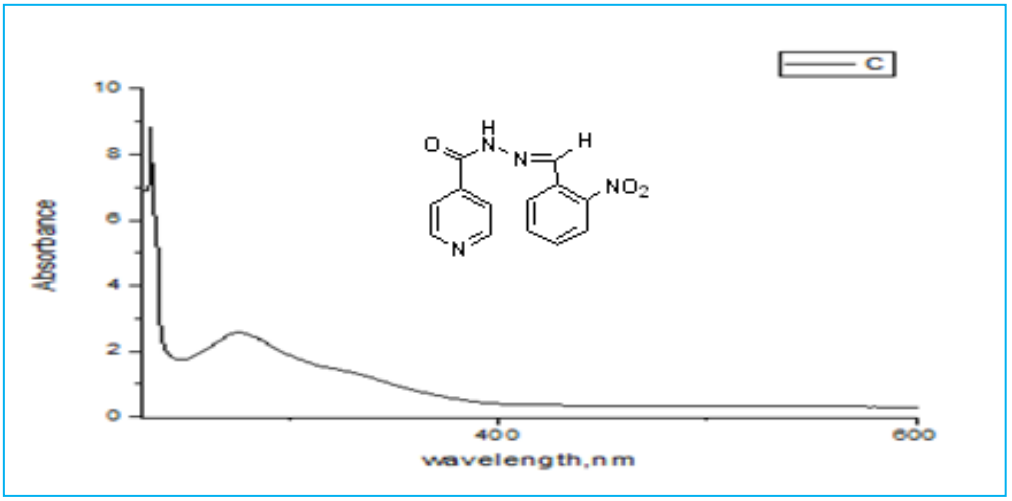

Figure S12. UV–Vis spectra of N-[(E)-(2-Nitrophenyl) methylen] isonicotinohydrazide (3c).

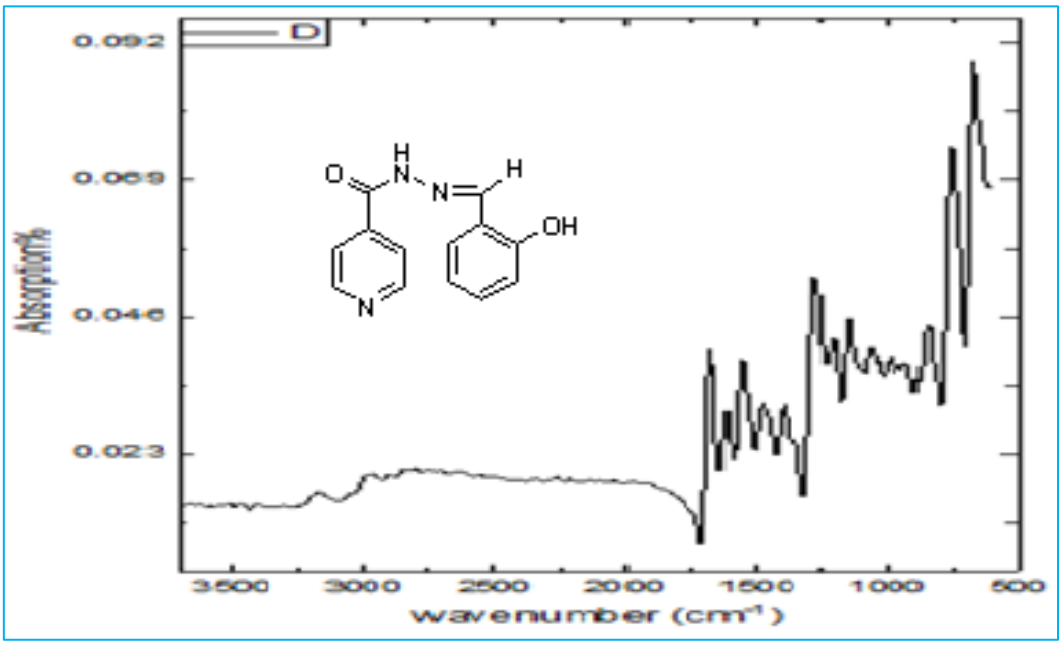

Figure S13. FT-IR spectra of N-[(E)-(2-Hydroxyphenyl) methylene] isonicotinohydrazide (3d).

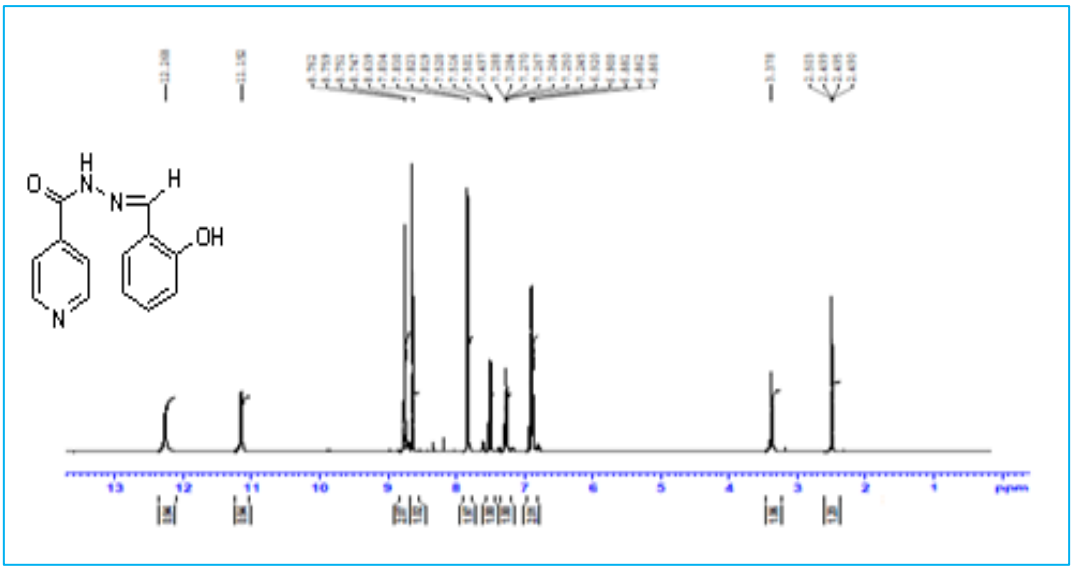

Figure S14. [1]H NMR spectra of N-[(E)-(2-Hydroxyphenyl) methylene] isonicotinohydrazide(3d).

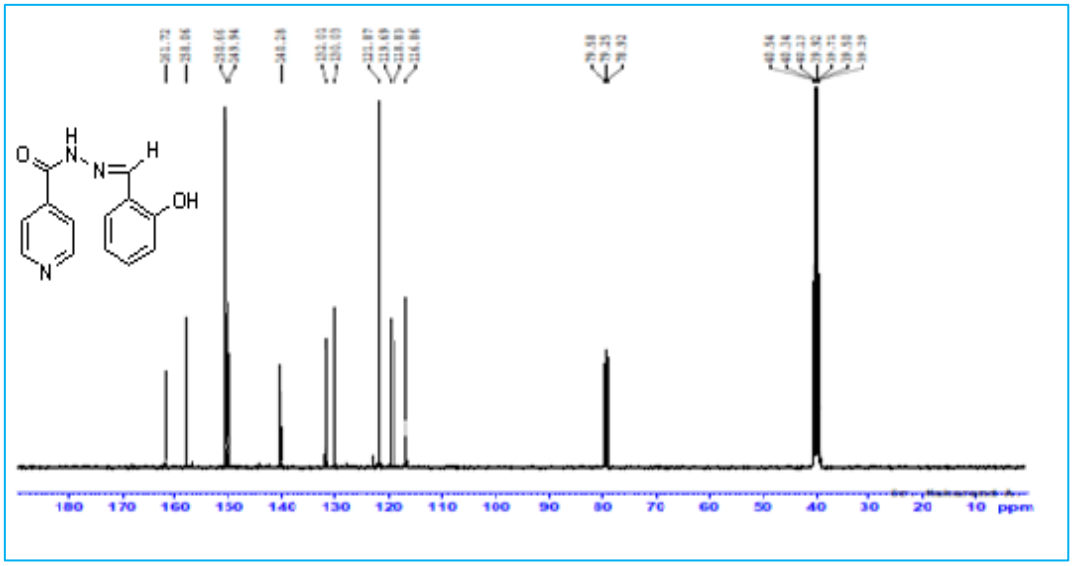

Figure S15. [13]CNMR spectra of N-[(E)-(2-Hydroxyphenyl) methylene] isonicotinohydrazide (3d).

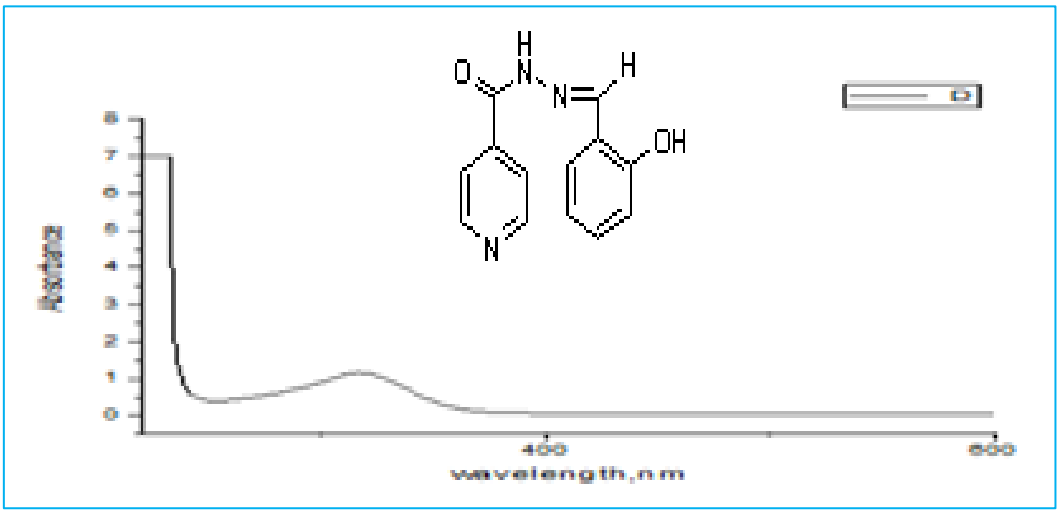

Figure S16. UV–Vis spectra of N-[(E)-(2-Hydroxyphenyl) methylen] isonicotinohydrazide(3d).

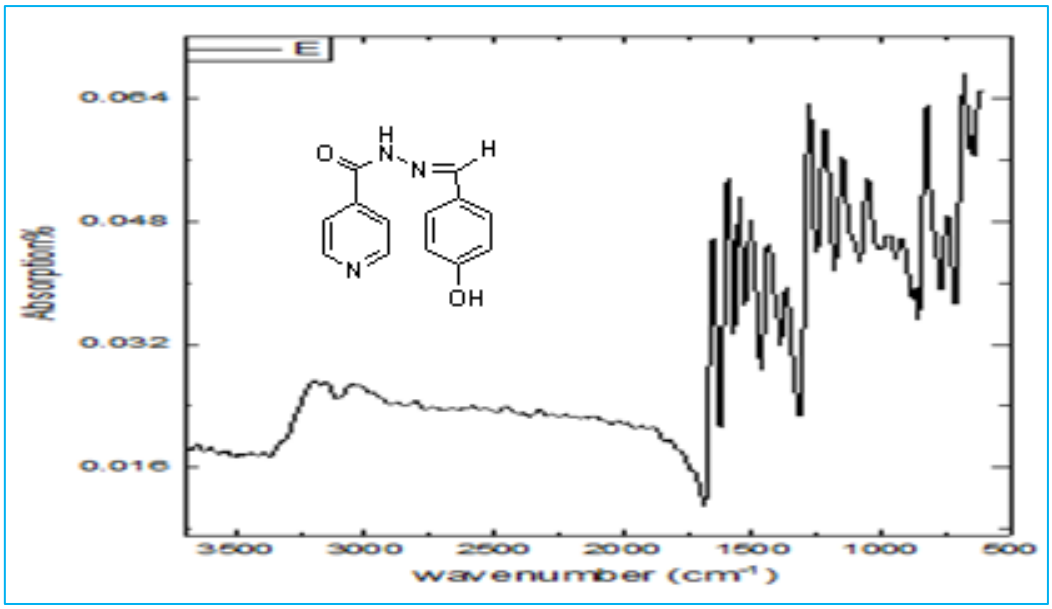

Figure S17. FT-IR spectra of N-[(E)-(4-Hydroxyphenyl) methylene] isonicotinohydrazide(3e).

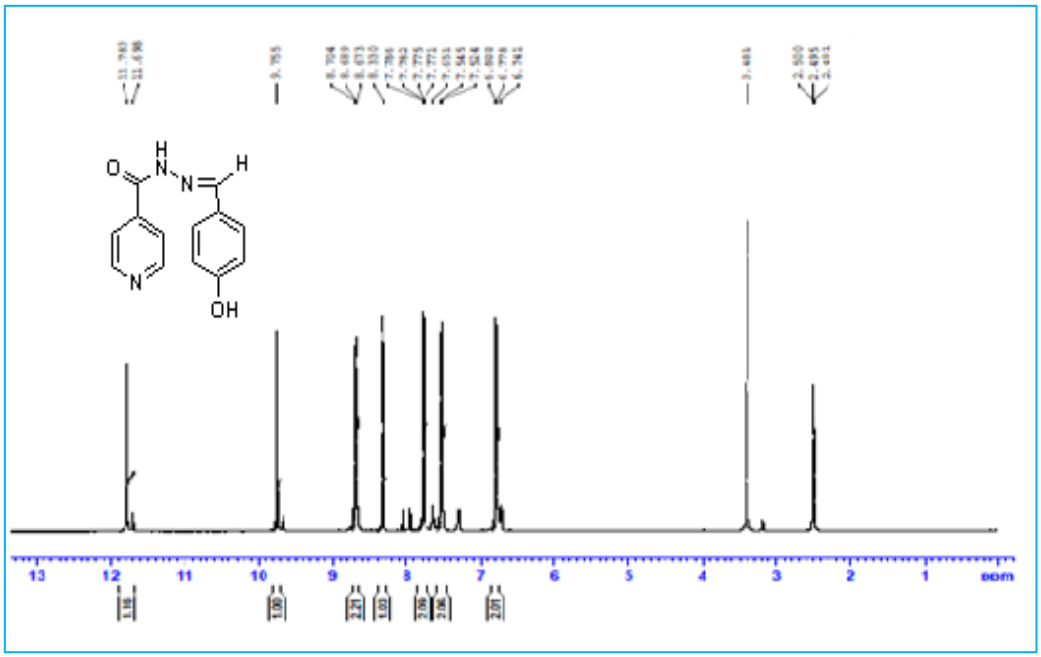

Figure S18. ^{1}H NMR spectra of N-[(E)-(4-Hydroxyphenyl) methylene] isonicotinohydrazide(3e).

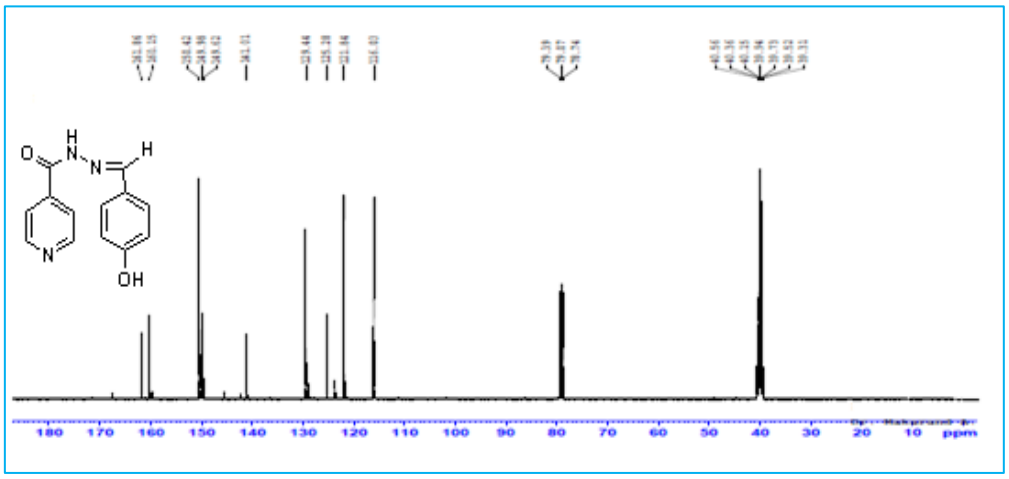

Figure S19. ^{13}CNMR spectra of N-[(E)-(4-Hydroxyphenyl) methylene] isonicotinohydrazide (3e).

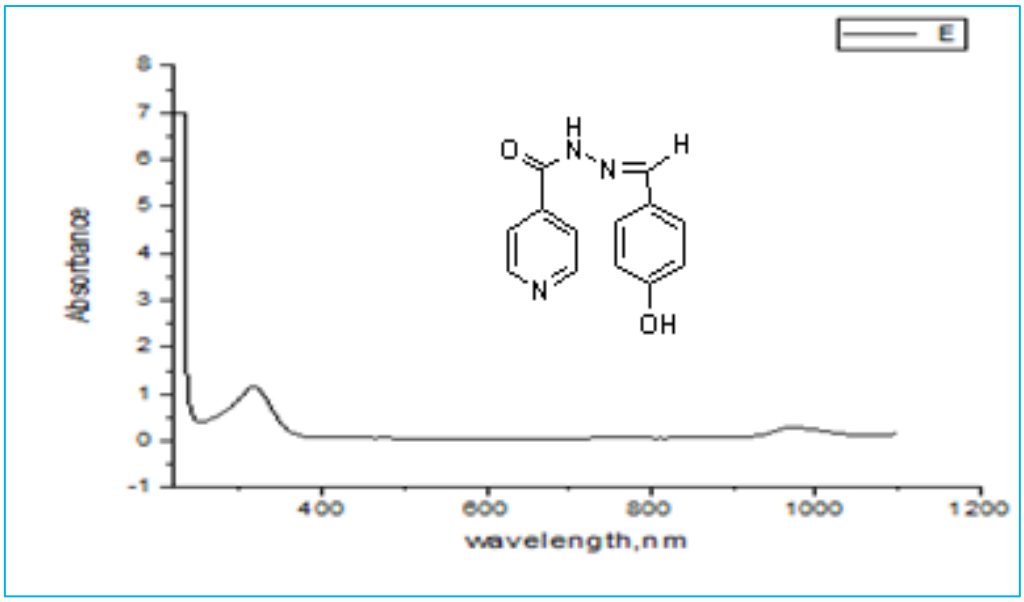

Figure S20. UV–Vis spectra N-[(E)-(4-Hydroxyphenyl) methylen] isonicotinohydrazide (3e).